DALTON
FULL PAPER

Ruthenium(II)/(III) bipyridine heterochelates incorporating phenolato imine functionalities. Synthesis, crystal structure, spectroscopic and electron-transfer properties and solution reactivities †

Soma Chakraborty, Mrinalini G. Walawalkar and Goutam Kumar Lahiri *

Department of Chemistry, Indian Institute of Technology, Bombay, Powai, Mumbai-400076, India

Received 29th February 2000, Accepted 15th June 2000
Published on the Web 25th July 2000

A new class of ruthenium–bipyridine complexes of the type $[Ru(bpy)_2(L')]ClO_4$ [bpy = 2,2′-bipyridine; L′ = $^-OC_6H_3(R)C(R')=NH$; R = R′ = H **1a**; R = H, R′ = CH_3 **1b**; R = NO_2, R′ = H **1c**] have been synthesized *via* cleavage of N–N and N–C (aliphatic and aromatic) bonds of binucleating imine functionalities. The formation of **1** has been authenticated by the single crystal structure determination of **1a**. The complexes exhibit strong MLCT transitions in the visible region and intraligand transitions in the UV region and display moderately strong emission near 700 nm. The quantum yield (φ) of the emission process at 77 K (EtOH–MeOH, 4 : 1 glass) varies in the range 2.2×10^{-2}–6.5×10^{-3} depending on L′ in **1**. The complexes show ruthenium(III)–ruthenium(II) and ruthenium(IV)–ruthenium(III) oxidations in the ranges 0.52–0.77 and 1.71–1.97 V *versus* SCE respectively. For **1a** and **1b**, one ligand centred oxidation near 2 V and for all the complexes two bipyridine based reductions have been detected in the ranges −1.51 to −1.56 V and −1.72 to −1.79 V *versus* SCE. Coulometric oxidation of **1** initially generates the unstable trivalent one-electron paramagnetic $[Ru^{III}(bpy)_2(L')]^{2+}$ congener, $\mathbf{1}^+$. The complexes $\mathbf{1}^+$ display one broad and moderately strong LMCT band near 750 nm and intraligand transitions in the UV region. The oxidised complexes $\mathbf{1}^+$ exhibit rhombic EPR spectra at 77 K which have been analysed to furnish values of distortion parameters (Δ = 4543–5923 cm^{-1}, V = 3251–5127 cm^{-1}) and energy of the expected ligand field transitions (ν_1 3086–3508, ν_2 6409–8669 cm^{-1}) within the t_2 shell. One of the ligand field transitions has been experimentally observed (ν_2 7092–7812 cm^{-1}). The oxidised species $\mathbf{1}^+$ slowly changes to diamagnetic dimeric species of the type $[(bpy)_2Ru^{III}\{^-OC_6H_3(R)C(R')=NNC(R')(R)C_6H_3O^-\}Ru^{III}(bpy)_2]^{4+}$ **2** where the ruthenium(III) centres are antiferromagnetically coupled. In the presence of water $\mathbf{1}^+$ as well as **2** return to the parent bivalent species **1**. The second order rate constants (k) of the conversion process $\mathbf{1}^+ \longrightarrow \mathbf{2}$ in dry acetonitrile and first order rate constants (k') of $\mathbf{1}^+ \longrightarrow \mathbf{1}$ in ordinary acetonitrile and the thermodynamic parameters ($\Delta H^{\ddagger}$ and $\Delta S^{\ddagger}$) of both have been determined spectrophotometrically in the temperature range 303–333 K.

Introduction

The discovery of important photo-redox activities of ruthenium–bipyridine complexes has generated continuous effort in the direction of designing new classes of these derivatives in order to develop efficient redox catalysts and photosensitisers.[1] The present trend in this direction has been tilted towards the framing of multinuclear to supramolecular ruthenium–bipyridine assemblies.[2] In that context we had begun a programme of co-ordinating two $Ru(bpy)_2$ units (bpy = 2,2′-bipyridine) through simple bridging ligands having anionic imine functionalities, H_2L^{1-12}, with varying lengths and electronic natures of the spacers. Although the bridging ligands H_2L are stable enough both in the solid and solution states, in contact with the precursor metal complex $[Ru(bpy)_2(EtOH)_2]^{2+}$ the N–N and N–C (aliphatic and aromatic) bonds of the linking units of H_2L^{1-12} are selectively cleaved. This in turn leads to the formation of a new class of ruthenium–bipyridine derivatives, $[Ru^{II}(bpy)_2(L')]^+$ **1**, where L′ corresponds to the stable imine functions $OC_6H_3(R)C(R')=NH$ incorporating the rare C=NH fragment. To the best of our knowledge this work demonstrates the first example of a stable imine moiety L′ having a (R)C=NH fragment attached to a metal centre, which so far is known only as an unstable intermediate.[3] Herein we report the synthesis of three such complexes, the crystal structure of one representative, their spectroscopic, electron-transfer properties and solution reactivites including kinetic studies.

† Electronic supplementary information (ESI) available: microanalytical data for ligands. See http://www.rsc.org/suppdata/dt/b0/b001663m/

Results and discussion

Synthesis

A group of twelve bridging ligands H_2L^{1-12} have been chosen for the present study. The ligands primarily differ with respect to the nature of the substituents (R/R′) present in the aldehydic and ketonic functions and the nature of the spacers (X). They are designed with the intention of holding two $Ru(bpy)_2$ units through the terminal O, N donors of L^{2-}. However, the reaction of H_2L with $[Ru^{II}(bpy)_2(EtOH)_2]^{2+}$ in ethanol solvent under a N_2 atmosphere results in monomeric complexes of the type $[Ru^{II}(bpy)_2(L')]^+$ **1** where L′ corresponds to an imine function of the type $^-OC_6H_3(R)C(R')=NH$. During the course of the reaction the N–N and N–C (aliphatic and aromatic) bonds of the bridging ligands H_2L are cleaved and the resulting monomeric fragment takes up a proton from the reaction medium which eventually leads to the formation of **1** (Scheme 1). The cleavage of the N–N and N–C bonds makes the four ligands in each set of R and R′ equivalent, thus the overall reactions essentially lead to the formation of three different complexes **1a**–**1c** (Scheme 1) which have been isolated as their perchlorate salts, $[Ru^{II}(bpy)_2(L')]ClO_4$.

DOI: 10.1039/b001663m

Table 1 Microanalytical,[a] conductivity,[b] IR [c] and electronic [b] spectral data

Compound	Microanalysis (%) C	H	N	Λ_M/Ω^{-1} cm^2 mol^{-1}	IR/cm^{-1} $\nu_{C=N}$	$\nu_{ClO_4^-}$	UV/vis λ/nm(ε/dm^3 mol^{-1} cm^{-1})
1a	51.02 (51.22)	3.40 (3.48)	11.21 (11.06)	145	1602	1091 623	578(2550),[d] 498(5050), 375(6300), 298(25850), 245(231500), 194(39300)
1b	51.88 (51.97)	3.67 (3.71)	10.95 (10.83)	148	1605	1105 631	574(5500),[d] 507(8500), 375(9300), 295(46950), 245(32800), 194(49900)
1c	47.97 (47.82)	3.17 (3.10)	12.54 (12.40)	140	1598	1110 630	534(6900),[d] 477(14400), 401(14300), 293(55850), 245(36550), 194(48300)
1a$^+$		—		—		—	1410(105), 790(1950), 358(4650), 314(11100), 271(19100), 210(41450), 194(54550)
1b$^+$		—		—		—	1280(85), 748(2450), 373(6600), 302(22750), 271(27050), 238(31450), 195(68650)
1c$^+$		—		—		—	1400(140), 680(2150), 364(10100), 313(31350), 244(41450), 202(82300)

[a] Calculated values are in parentheses. [b] In acetonitrile solution. [c] As KBr discs. [d] Shoulder.

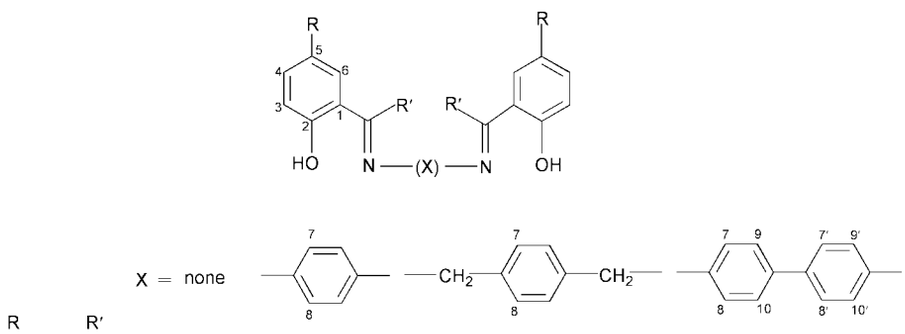

R	R′	X = none			
H	H	H_2L^1	H_2L^2	H_2L^3	H_2L^4
H	CH_3	H_2L^5	H_2L^6	H_2L^7	H_2L^8
NO_2	H	H_2L^9	H_2L^{10}	H_2L^{11}	H_2L^{12}

$$[Ru^{II}(bpy)_2(EtOH)_2]^{2+} + H_2L \xrightarrow{(i)} [Ru^{II}(bpy)_2(L')]^+$$

$H_2L^{1-4} \longrightarrow$ **1a**

$H_2L^{5-8} \longrightarrow$ **1b**

$H_2L^{9-12} \longrightarrow$ **1c**

Scheme 1 (i) EtOH, $NaOCH_3$, N_2, stirring, 298 K.

Under identical reaction conditions (Scheme 1) but in the absence of metal precursor the binucleating identity of H_2L remains unaltered even upon heating. This implies direct involvement of the $Ru(bpy)_2^{2+}$ core in driving the reaction equilibrium in the direction of products **1**.

The complexes **1** are highly soluble in CH_3CN, DMF, DMSO and moderately soluble in CH_2Cl_2, $CHCl_3$ and slightly in water. Their microanalytical data are in good agreement with the calculated values (Table 1). The complexes act as 1:1 electrolytes in acetonitrile solution (Table 1) and are diamagnetic at room temperature. Selected IR bands are listed in Table 1. The C=N stretching frequencies of the "free" ligands (≈1640 cm^{-1}) have been shifted to ≈1600 cm^{-1} in the complexes in accordance with co-ordination of the azomethine (CH=N) function. The bands due to ionic perchlorate and NH function are observed near 1100/625 and 3300 cm^{-1} respectively (Table 1).

Crystal structure of $[Ru^{II}(bpy)_2(L')]ClO_4 \cdot CH_3CN$ 1a

The formation of complexes **1** has been authenticated in one case, **1a**, by single-crystal structure determination. The structure is shown in Fig. 1 and selected bond distances and angles are listed in Table 2. The single crystal contains acetonitrile of crystallisation in the ratio **1a**:CH_3CN = 1:1. The RuN_5O co-ordination sphere is distorted octahedral as can be seen from the angles subtended at the metal. The *cis* angles around the metal ion range from 78.58(15) to 100.50(13)° with an average

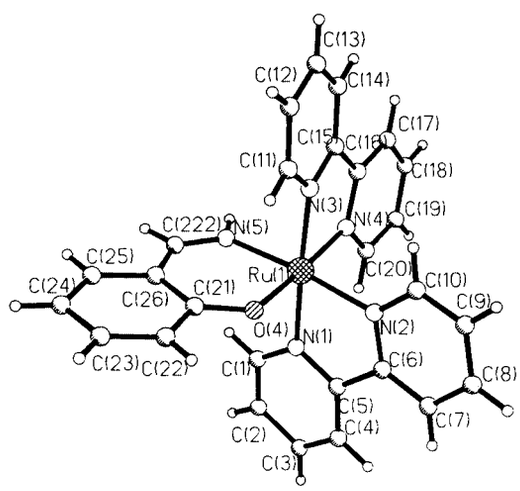

Fig. 1 Crystal structure of complex **1a**. The perchlorate anion and acetonitrile molecule are removed for clarity.

value of 90.06(14)°. The average *trans* angle is 174.41(14)°. The distortion of the co-ordination sphere is primarily caused by the two acute (≈78°) bite angles of the juxtaposed two bipyridine chelate rings. The bite angle of the phenolato imine chelate, 91.70(13)°, is very close to the ideal value. The ruthenium–phenolato moiety is essentially planar. The Ru^{II}–O distance is observed to be 2.060(3) Å which agrees well with the Ru^{II}–O (phenolato) distance 2.064(4) Å observed in $[Ru^{II}(bpy)_2(NC_5H_4C_6H_4O)]^+$ [4] but slightly longer than the 2.022(5) and 2.042(4) Å observed in $[Ru^{II}(tap)_2(cat)]$ [5] (tap = tolylazopyridine, cat = catecholate) and $[Ru^{II}(bpy)_2(sal)]$ [6] (sal = salicylate) respectively. However, it is much shorter than the Ru^{II}–O distances found in $Ru^{II}O(H_2O)$, 2.122(16) Å,[7] and Ru^{II}–

Table 2 Selected bond distances (Å) and angles (°) and their estimated standard deviations for $[Ru(bpy)_2(L')]ClO_4 \cdot CH_3CN$ **1a**

Ru–N(1)	2.046(4)	Ru–O(4)	2.060(3)
Ru–N(2)	2.009(4)	C(222)–N(5)	1.280(6)
Ru–N(3)	2.050(4)	C(21)–O(4)	1.302(6)
Ru–N(4)	2.033(4)	C(1)–C(2)	1.356(9)
Ru–N(5)	2.039(4)	N(1)–C(1)	1.353(6)
N(2)–Ru–N(4)	92.92(15)	N(5)–Ru–N(3)	84.76(15)
N(2)–Ru–N(1)	78.94(14)	N(2)–Ru–O(4)	86.05(15)
N(4)–Ru–N(1)	97.53(15)	N(4)–Ru–O(4)	172.77(14)
N(2)–Ru–N(5)	174.41(13)	N(1)–Ru–O(4)	89.30(14)
N(4)–Ru–N(5)	89.96(15)	N(5)–Ru–O(4)	91.70(13)
N(1)–Ru–N(5)	95.94(15)	N(3)–Ru–O(4)	94.55(14)
N(2)–Ru–N(3)	100.50(13)	C(222)–N(5)–Ru	124.0(3)
N(4)–Ru–N(3)	78.58(15)	C(21)–O(4)–Ru	125.2(3)
N(1)–Ru–N(3)	176.06(15)		

O(phenolato) in four-membered metallocycles, 2.235(4)[8] and 2.205 Å.[9] It may be noted that only a limited number of authentic Ru^{II}–O(phenolato) distances are available in the literature.

The observed three ruthenium–nitrogen (bipyridine) bond lengths of 2.033(4), 2.046(4) and 2.050(4) Å agree well with values found in other bivalent ruthenium–bipyridine complexes, however Ru–N(2) (2.009 Å) is significantly shorter.[6]

The Ru–N(5) (imine nitrogen) distance in complex **1a** is 2.039(4) Å, which merits scrutiny. No information on Ru–N (imine nitrogen) bond lengths is available in the literature, but Ru^{II}–N (oxime nitrogen) distances have been observed to be 1.989(7) and 1.986(7) Å.[10] The present relatively long Ru–N(5) distance may account for the significantly short Ru–N(2) bond length. The bond distance of N(5)–C(222) is 1.280(6) Å, which is normal for a C=N double bond.[8] The four oxygen atoms of the perchlorate anion are thermally disordered and were refined anisotropically giving partial occupancy for each. The ClO_4^- anion is tetrahedral with an average Cl–O distance of 1.337 Å and an average O–Cl–O angle of 109.45°.

The protonation of the imine function in complex **1a** is confirmed by the ^{1}H NMR spectrum (see later).

^{1}H NMR spectra

The ^{1}H NMR spectra of one set of ligands (H_2L^1–H_2L^4, where R = R′ = H) have been recorded in $(CD_3)_2SO$ solvent. The data are listed in Table 3 and representative spectra are shown in Fig. 2. The observed ^{1}H NMR spectra of H_2L^{1-3} (Fig. 2a) indicate that each half of the ligand is equivalent due to internal symmetry, therefore it may be assumed that the *trans* configuration of the ligands is predominant in solution or that there is a fast equilibrium between the *cis* and *trans* isomers of H_2L^{1-3}. In the case of H_2L^4 the preferred *trans* configuration of the two phenyl rings of the biphenyl group[11] makes each half of the ligand different. However, except for H-9/10 and H-9′/10′ all aromatic protons are found to overlap (Table 3, Fig. 2b).

The ^{1}H NMR spectra of complexes **1a**–**1c** were recorded in $(CD_3)_2SO$, and a representative is shown in Fig. 2(c). The absence of the OH proton of the "free" ligands H_2L ($\delta \approx 11$–12, Table 3) in the spectra of the complexes suggests metallation through the phenolato oxygen. The presence of asymmetric ligands L'^- assures non-equivalence of all aromatic rings. The molecules **1a/1b** and **1c** thus possess twenty and nineteen non-equivalent aromatic protons respectively. Since the electronic environments of many aromatic hydrogen atoms are very similar, their signals may appear in a narrow chemical shift range. In fact the aromatic regions of the spectra are complicated, however direct comparisons of the intensity of the aromatic proton signals with that of the clearly observable singlet due to the CH=N proton for complexes **1a** and **1c** ($\delta \approx 9$) and the singlet of the methyl group ($\delta \approx 2.39$) for **1b** reveal the presence of the calculated number of aromatic protons. The partial overlapping of the signals makes it difficult to assign all

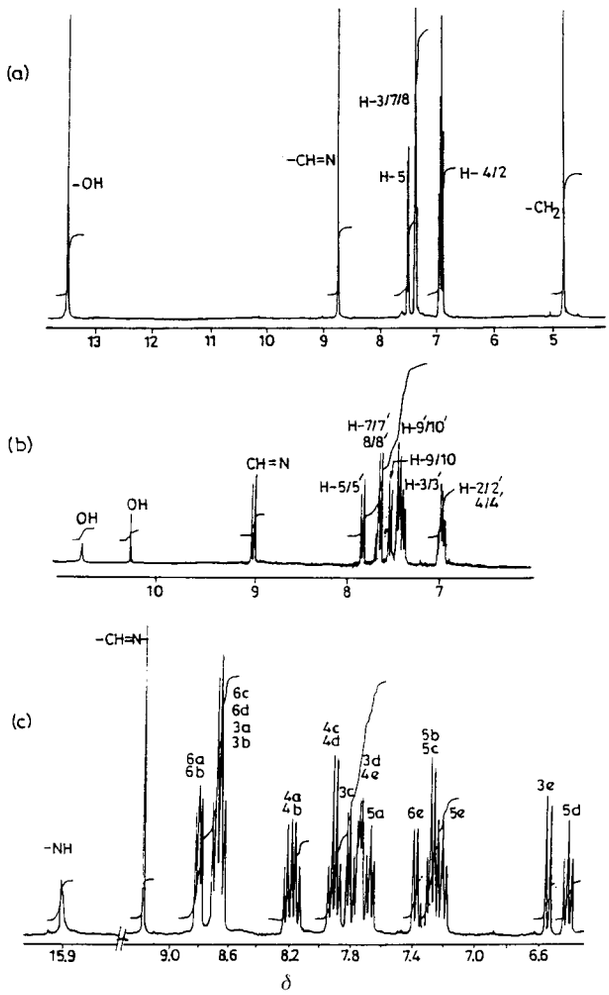

Fig. 2 ^{1}H NMR spectra of (a) H_2L^3, (b) H_2L^4 and (c) complex **1a** in $(CD_3)_2SO$.

the individual signals, but with the help of ^{1}H correlation spectroscopy (COSY) the observed twenty aromatic signals for **1a** and **1b** could be separated into five groups of four each, and for **1c** four groups of four each and one group of three protons corresponding to H^3, H^4, H^5 and H^6 of the aromatic ring (usual numbering).

In the complexes the equatorial plane contains one pyridine ring from each of the two bipyridine ligands (b,d), the oxygen atom and the azomethine nitrogen atom of the ligand (L'^-). The axial positions are occupied by the other pyridine ring of the bipyridine ligands. The signals of the pyridine ring (d) which is *trans* to the phenolato oxygen are likely to be different from the rest since they experience the *trans* effect of the σ-donor phenolato function. Therefore the signal which appears most upfield for the individual H^6, H^5, H^4, H^3 may be assigned to the corresponding d ring. The order of the pyridine ring protons in increasing field strength appears to be 6 > 3 > 4 > 5 for rings a and b but for pyridine rings c and d it is 6 > 4 > 3 > 5. It may be noted that similar distribution patterns of pyridine ring protons have been observed for other $[Ru(bpy)_2L]$ systems where L corresponds to an asymmetric ligand.[4] Of the four bipyridine pyridine rings (a–d), except for the d-ring protons, the other sets cannot be assigned unambiguously to particular pyridine rings. The phenolato imine function protons follow the order 4 > 6 > 5 > 3 for **1a** and **1c** but for **1b** it is 6 > 4 > 5 > 3. The effects of the presence of the σ-donating phenolato function and of the electron withdrawing NO_2 group in the ring 'e' are directly reflected in the relative chemical shifts of the ring 'e' signals.

The protonation of the azomethine function in complex **1** is confirmed by ^{1}H NMR spectra. The NH proton signal is

Table 3 ^{1}H NMR spectral data of ligands H_2L^1–H_2L^4 in $(CD_3)_2SO$

Ligand	δ(*J*/Hz)[a]										
	H(2)	H(3)	H(4)	H(5)	H(7)	H(8)	H(9)	H(10)	CH_2	CH=N	OH
H_2L^1	7.03 (8.0)[b]	7.39 (8.0)[c]	6.97 (7.5)[c]	7.35 (8.5)[b]	—	—	—	—	—	8.70[d]	11.40[d]
H_2L^2	6.96 (7.8)[b]	7.46 (7.2)[c]	6.99 (8.1)[c]	7.67 (8.1)[b]	7.41 (7.9)[b]	7.41 (7.9)[b]	—	—	—	8.98[d]	12.90[d]
H_2L^3	6.87 (7.5)[b]	7.33 (7.8)[c]	6.91 (7.7)[c]	7.48 (6.8)[b]	7.36 (7.1)[b]	7.36 (7.1)[b]	—	—	4.8[d]	8.87[d]	13.41[d]
H_2L^4	6.96 (7.9)[b]	7.41 (8.2)[c]	7.0 (7.7)[c]	7.85 (8.4)[b]	7.69 (8.1)[b]	7.65 (7.6)[b]	7.54 (8.3)[b] 7.46 (8.5)[b]	7.54 (8.3)[b] 7.46 (8.5)[b]		9.05[d] 9.01[d]	10.74[d] 10.26[d]

[a] Tetramethylsilane as internal standard. [b] Doublet. [c] Triplet. [d] Singlet.

observed near δ 16 (for **1a**, 16; **1b**, 15.8; **1c**, 15.87) and integrates to one proton, which as expected disappears upon D_2O treatment.[8,9,12]

Electronic spectra

Electronic spectral data of the complexes **1** in acetonitrile solvent are given in Table 1 and spectra are shown in Fig. 3. Multiple transitions in the UV-visible region are due to the presence of different acceptor levels. In the visible region the complexes display two transitions near 500 and 400 nm. The lower energy transition (≈500 nm) is associated with a shoulder at lower energy.

The two visible bands have been assigned on the basis of reported spectra of $[Ru(bpy)_2]^{2+}$ complexes having other types of chelated third ligands.[13] The bands near 500 and 400 nm are considered to be $d\pi(Ru^{II}) \longrightarrow \pi^*(\Psi)$ and the $d\pi(Ru^{II}) \longrightarrow \pi^*(\chi)$ MLCT transitions respectively where $\pi^*(\Psi)$ and $\pi^*(\chi)$ are believed to be antisymmetric and symmetric bipyridine acceptor orbitals respectively. The bands in the UV region are of intraligand π–π* type or charge transfer transitions involving levels which are higher in energy than those of the ligand lowest unoccupied molecular orbital (LUMO).

The lowest energy MLCT transition of $[Ru^{II}(bpy)_3]^{2+}$ appears at 450 nm,[14] therefore replacement of one bpy ligand by an asymmetric ligand (L'^-) results in a red-shift of the same transition. The lower ligand-field strength of σ-donating L'^- compared to the π-acceptor bpy ligand and overall lowering of the molecule symmetry on moving from $Ru(bpy)_3^{2+}$ to **1** are the contributing factors for the observed trend. Other known ruthenium(II)–bis-bipyridine systems having RuN_5O chromophores, $[Ru^{II}(bpy)_2L]^+$, L = pyridine-2-phenolate or pyridine-2-olate, exhibit lowest-energy MLCT transitions at 570 and 500 nm respectively.[4,15] Thus the present set of complexes **1** appear to be similar to pyridine-2-olate complexes as far as the ligand field is concerned.

Emission spectra

Excitation of complexes **1** at the lowest energy MLCT bands in 1:4 MeOH:EtOH glass at 77 K results in emissions near 700 nm (Table 4, Fig. 3). The origin of the emission spectra is further confirmed by the excitation spectra of corresponding solutions. For all three cases one luminescence band and a single exponential decay are observed as expected from triplet MLCT emission of ruthenium(II)–bipyridine complexes.[16]

The quantum yields of the complexes were determined by comparison with the reported quantum yield of $[Ru(bpy)_3]^{2+}$ in 1:4 MeOH:EtOH glass at 77 K ($\varphi_{em,s} = 0.35$).[17] For the calculations, the excitation wavelengths were chosen such that the standard reference and sample absorptions are equal. The quantum yield φ was calculated by following the reported method,[18] eqn. (1), where A_s, A_r are the absorption values of

Table 4 Emission data[a]

Compound	λ_{max}/nm		Quantum yield (φ)[b]
	excitation	emission	
1a	488	688	6.3×10^{-3}
1b	506	703	2.2×10^{-2}
1c	475	676	6.5×10^{-3}

[a] In MeOH–EtOH 1:4 at 77 K. [b] Calculated by using eqn. (2).

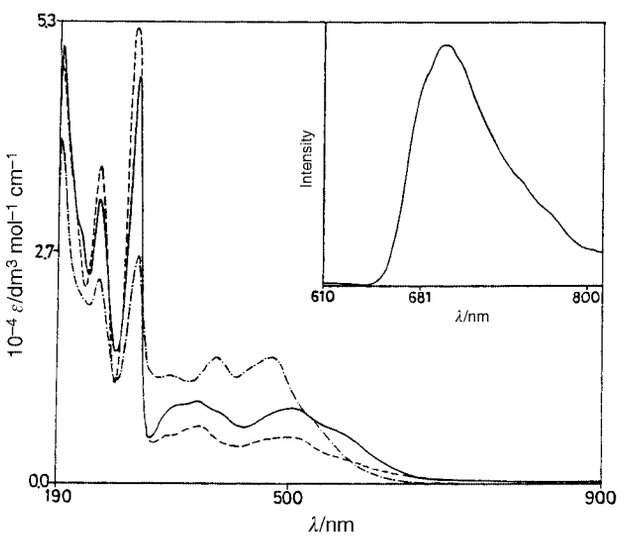

Fig. 3 Electronic spectra of complexes **1a** (-----), **1b** (———) and **1c** (–·–·–·–) in acetonitrile. The inset shows the emission spectrum of **1b** in EtOH–MeOH 4:1 (v/v) at 77 K.

$$\varphi_{em,s} = \varphi_{em,r}(A_r/A_s)(I_s/I_r)(n_s/n_r)^2 \quad (1)$$

sample and reference, I_s, I_r their emission intensities and n_s, n_r their refractive indices. Since A_s and A_r are equal and the refractive indices are assumed to be similar, eqn. (1) can be modified to (2). The calculated quantum yields for the com-

$$\varphi_{em,s} = \varphi_{em,r}(I_s/I_r) \quad (2)$$

plexes are listed in Table 4. Complex **1b** having a keto-based imine function exhibits the strongest emission, **1b** > **1a** > **1c**.

The red shift of the emission maximum while moving from $Ru(bpy)_3^{2+}$ to the present complexes **1a**–**1c** is consistent with the electrochemical results (see later). The emission energy increases with increasing redox energy, the difference in energy between the metal centred oxidation process and the first ligand centred reduction of the complexes. The introduction of a σ-donor imine function (L'^-) instead of a strong π-acidic bpy

Table 5 Electrochemical data in acetonitrile at 298 K [a]

Compound	E°_{298}/V (ΔE_p/mV)				ΔE° [b]/V	ν_{MLCT}/cm^{-1}	
	Ru^{III}–Ru^{II} Couple	Ru^{IV}–Ru^{III} oxidation	Ligand oxidation	Ligand reduction		obs.[d]	calc.[e]
1a	0.61 (70)	1.86[c]	2.36[c]	−1.51 (70) −1.74 (95)	2.12	20098	20576
1b	0.518 (80)	1.71[c]	2.25[c]	−1.56 (70) −1.79 (100)	2.08	19775	19762
1c	0.770 (80)	1.97[c]	—	−1.54 (80) −1.72 (100)	2.31	21630	21052

[a] Solvent, acetonitrile; supporting electrolyte, NEt_4ClO_4; reference electrode, SCE; solute concentration, $\approx 10^{-3}$ mol dm^{-3}; working electrode, platinum. Cyclic voltammetric scan rate, 50 mV s^{-1}; $E^\circ_{298} = 0.5(E_{pc} + E_{pa})$ where E_{pc} and E_{pa} are cathodic and anodic peak potentials respectively. [b] Calculated by using eqn. (4) of text. [c] E_{pa} values, due to irreversible nature of the voltammograms. [d] In acetonitrile solution. [e] Using eqn. (3) of text.

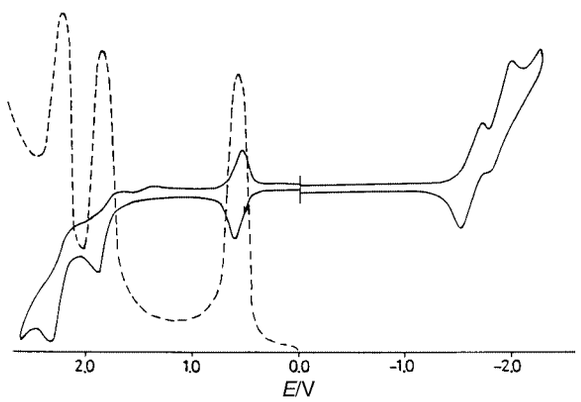

Fig. 4 Cyclic voltammograms of a $\approx 10^{-3}$ mol dm^{-3} solution of complex **1a** in acetonitrile at 298 K. Differential pulse voltammograms are shown only for positive potentials.

ligand in the $Ru(bpy)_2$ core lowers the energy of the e_g orbitals and hence narrows the energy gap between the MLCT and d–d states. The d–d state therefore becomes thermally accessible and decays through an alternative route. This is reflected in the lower φ values of **1** as compared to $Ru(bpy)_3^{2+}$.

Electrochemical studies

The electrochemical properties of complexes **1** have been studied in acetonitrile solution by cyclic voltammetry and constant-potential coulometry using a platinum working electrode. The complexes are electroactive with respect to the metal as well as the ligand centres and display five redox processes in the potential range ±2.5 V *versus* SCE. Representative voltammograms are shown in Fig. 4 and the data are summarised in Table 5.

The complexes display one reversible oxidation process which is assigned to the ruthenium(III)–ruthenium(II) couple. The one-electron nature of the couple is confirmed by constant-potential coulometry (Table 5). The presence of trivalent ruthenium in the oxidised solution of $\mathbf{1}^+$ has been confirmed by the characteristic EPR spectra of the ruthenium(III) congeners (see later).[15] The formal potential of the ruthenium(III)–ruthenium(II) couple varies depending on L′, such that the electron-donating methyl group in **1b** decreases the potential and the electron-withdrawing NO_2 group in **1c** increases it with respect to that of complex **1a** (Table 5).

Thus substitution of one π-acidic bpy ligand from the $[Ru(bpy)_3]^{2+}$ core by one σ-donating L′ in complexes **1** results in a decrease of the ruthenium(III)–ruthenium(II) potential. This is due to the reduction of overall charge of the complex cation from +2 in $[Ru(bpy)_3]^{2+}$ to +1 in **1** which provides electrostatic stabilisation of the oxidised Ru^{III}–L′ species.

Other RuN_5O chromophoric systems, $[Ru^{II}(bpy)_2(L'')]$ (L″ = pyridine-2-phenolate or -olate) exhibit the ruthenium(III)–ruthenium(II) couple at 0.41 and 0.64 V respectively.[4,15] The similarity of the ruthenium(III)–ruthenium(II) potential of **1a** with that of the pyridine-2-olate system further supports the close ligand field strengths of these two classes of complexes.

Complexes **1** also display a second irreversible oxidation process. The one-electron nature of this is confirmed by differential pulse voltammetry. It could be due to either $Ru^{III} \longrightarrow Ru^{IV}$ oxidation or oxidation of the ligand. The potential difference between the two successive oxidation processes is ≈1.2 V, which agrees well with the average potential difference between the redox processes of the ruthenium centre ($Ru^{II/III} - Ru^{III/IV}$) (≈1.0–1.5 V) observed in other mononuclear complexes.[19] Therefore we believe that the second redox process corresponds to ruthenium(III)–ruthenium(IV) oxidation. The formal potentials are found to vary in the expected manner depending on the electronic nature of L′.

The complexes **1a** and **1b** also exhibit a third irreversible oxidation process above 2 V. In the case of **1c** the third oxidation process could not be seen within the experimental potential limit +2.5 V possibly due to solvent cut off. Although the anodic current height (i_{pa}) of this irreversible process is ≈1.5 times that of the previous redox processes, Ru^{III}–Ru^{II} and Ru^{IV}–Ru^{III}, the differential pulse voltammogram shows the third oxidation wave to have the almost same height, implying a one-electron process. The third oxidative response might be due either to oxidation of the ligand L′ or to $Ru^{IV} \longrightarrow Ru^{V}$ oxidation. Since the redox behaviour of L′ either in the free state or in other complex systems has not been investigated, it is difficult to rule out one particular possibility exclusively. However, a ligand based response seems appealing as ruthenium(V) complexes are known to be rare particularly in non-oxo environments.

Two successive one-electron reductions due to co-ordinated bpy are also observed for all the complexes (Fig. 4, Table 5).[4,15]

Spectroelectrochemical correlation

The observed MLCT transitions for complexes **1** involve the excitation of an electron from the filled t_{2g}^6 orbital of ruthenium(II) to the lower π* orbital of the diimine function of bpy. The energy of this band can be predicted from the observed electrochemical data with the help of eqns. (3) and (4).[20]

$$\nu_{MLCT} = 8065(\Delta E^\circ) + 3000 \quad (3)$$

$$\Delta E^\circ = E^\circ_{298}(Ru^{III}\text{–}Ru^{II}) - E^\circ_{298}(L') \quad (4)$$

$E^\circ_{298}(Ru^{III}\text{–}Ru^{II})$ corresponds to formal potential (in V) of the Ru^{III}–Ru^{II} couple, $E^\circ_{298}(L')$ that of the first ligand reduction and ν_{MLCT} is the frequency or energy of the charge-transfer band in cm^{-1}. The factor 8065 is used to convert the potential difference ΔE from V into cm^{-1} and the term 3000 cm^{-1} is of empirical origin. The calculated and experimentally observed ν_{MLCT} values are listed in Table 5 and are in exceptionally good agreement.

Table 6 EPR g values,[a] distortion parameters[b] and NIR transitions[c]

Compound	g_x	g_y	g_z	k	Δ/λ	V/λ	ν_1/λ	ν_2/λ	ν_2/λ (obs.[c])
$\mathbf{1a}^+$	−2.340	−2.080	1.854	0.594	5.391	−4.167	3.456	7.676	7.092
$\mathbf{1b}^+$	−2.333	−2.061	1.867	0.586	5.923	−5.127	3.508	8.669	7.812
$\mathbf{1c}^+$	−2.300	−2.051	1.812	0.484	4.543	−3.251	3.086	6.409	7.142

[a] Measurements were made in acetonitrile at 77 K. [b] Symbols have the same meaning as in the text. [c] In acetonitrile.

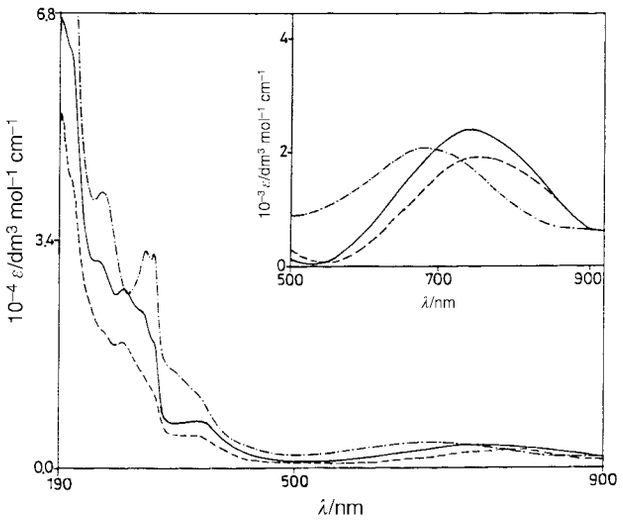

Fig. 5 Electronic spectra of complexes $\mathbf{1a}^+$ (-----), $\mathbf{1b}^+$ (———) and $\mathbf{1c}^+$ (–·–·–·–) in acetonitrile. The inset shows the expanded part of the spectra in the range 500–900 nm.

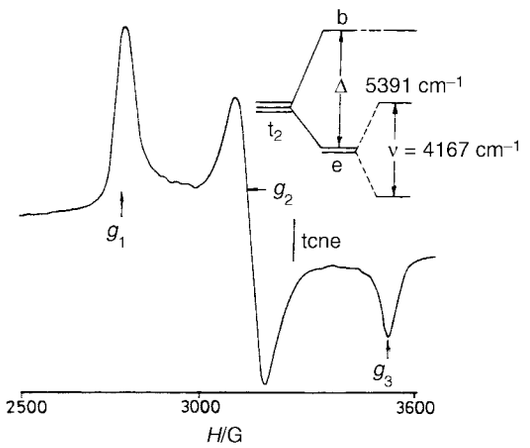

Fig. 6 X-Band EPR spectrum and t_2 splittings of complex $\mathbf{1a}^+$ in acetonitrile–toluene at 77 K.

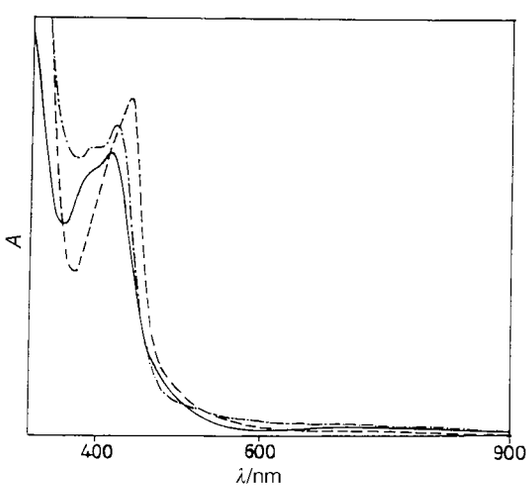

Fig. 7 Qualitative electronic spectra of complexes **2a** (–––), **2b** (———) and **2c** (—·—) in acetonitrile.

Electrogeneration of trivalent ruthenium congeners 1^+, distortion parameters and solution properties

Coulomeric oxidations of complexes **1a**–**1c** in dry acetonitrile solvent at a potential of ≈200 mV above the E_{pa} of the first oxidation couple generate a deep green oxidised solution. The observed coulomb count corresponds to one-electron transfer for each case (Table 5). The resulting oxidised solution shows cyclic voltammograms which are identical to those of the starting bivalent complexes, $[Ru^{II}(bpy)(L')]^+$, this may be due to the stereoretentive nature of the oxidation process. The oxidised solution can quantitatively be reduced to the parent bivalent state. In the visible region the complexes $\mathbf{1}^+$ exhibit one moderately intense broad band near 750 nm (Table 1, Fig. 5) corresponding to $\pi(bpy) \longrightarrow t_{2g}(Ru^{III})$ LMCT transition.[4] The X-band EPR spectra of $\mathbf{1}^+$ in acetonitrile (produced coulometrically followed by quick freezing in liquid N_2, 77 K) are rhombic characteristic of low-spin ruthenium(III) complexes in distorted octahedral environments (Table 6, Fig. 6).[21] The EPR spectra were analysed using the g-tensor theory for low-spin d^5 ions.[22] This afforded values of the axial distortion (Δ) which splits the t_2 shell into e + b and of the rhombic distortion (V) which splits e further into two non-degenerate components. The value of the orbital reduction factor k is also furnished by analysis. Two ligand field transitions ν_1 and ν_2 among the Kramer's doublets are expected. Their energies, along with values of Δ and V calculated from the g parameters with help of the theory, are listed in Table 6. The spin–orbit coupling constant, λ, of Ru^{III} was taken as 1000 cm^{-1}.[23] In near-IR spectra the ν_2 band is indeed detected in the expected position (Table 6). In view of the approximation involved in the theory, the agreement between the experimentally observed and calculated ν_2 value is excellent. Owing to the instrumental wavelength scan limitation (maximum up to 2200 nm) it has not been possible to check the ν_1 band. The presence of a high degree of distortion in the complexes $\mathbf{1}^+$ is reflected in the Δ and V values (Table 6). The complexes behave as model ruthenium(III) species possessing rhombic symmetry.

The coulometrically oxidised complexes $\mathbf{1a}^+$–$\mathbf{1c}^+$ are found to be unstable. In dry acetonitrile solvent the oxidised deep green one-electron paramagnetic $\mathbf{1}^+$ slowly changes to an EPR silent diamagnetic species. The intensity of the LMCT band of $\mathbf{1}^+$ near 750 nm gradually decreases with the concomitant growth of a new band near 430 nm and eventually it transforms to a yellowish green species having a completely different spectral profile (Table 1, Fig. 7). On the other hand in the presence of a small amount of water (ordinary acetonitrile) the oxidised $\mathbf{1}^+$ gradually reduces to the parent bivalent species **1**.

However, the direct addition of water to a dry acetonitrile solution of $\mathbf{1}^+$ accelerates the reduction process. Thus the rate of conversion of $\mathbf{1}^+ \longrightarrow \mathbf{1}$ is dependent on the water content in acetonitrile. The transformed yellowish green species exhibits two closely spaced reversible ruthenium(III)–ruthenium(II) reduction couples almost at the same potential as that of the starting deep green $\mathbf{1}^+$ (Fig. 8). Considering all the facts together it may be reasonable to believe that in dry acetonitrile solution the electrochemically generated trivalent monomeric species $\mathbf{1}^+$ dimerises to a diamagnetic species of

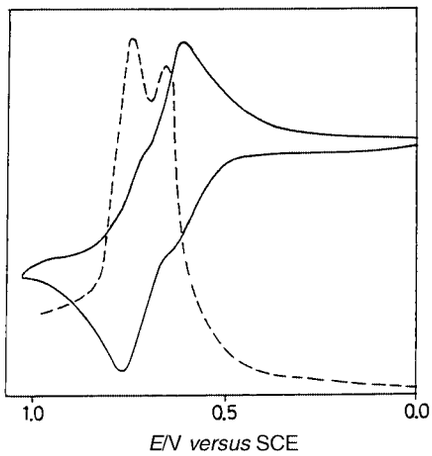

Fig. 8 Cyclic voltammogram and differential pulse voltammogram of coulometrically generated complex **2a** in acetonitrile at 298 K (only Ru^{III}–Ru^{II} couples are shown).

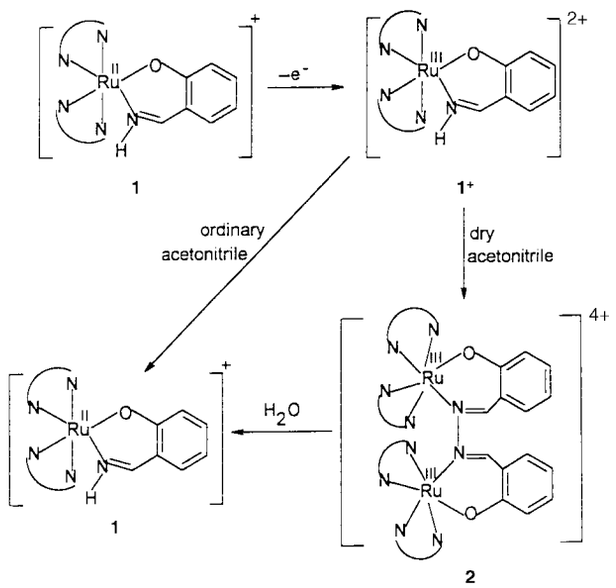

Scheme 2

type **2** (Scheme 2) where the two ruthenium(III) centres are antiferromagnetically coupled.[24] In contact with water the N–N bond of **2** is cleaved which in turn leads to the formation of the parent monomeric species **1**. The observed instability of $\mathbf{1}^+$ and **2** in the presence of water may account for the formation of mononuclear complexes **1** starting from the binucleating ligands H_2L (Scheme 1). The two closely spaced cyclic voltammetric responses of **2** (Fig. 8) are assigned to successive reductions of two ruthenium(III) centres, eqns. (5) and (6).

$$Ru^{III}\text{–}Ru^{III} + e^- \longrightarrow Ru^{III}\text{–}Ru^{II} \quad (5)$$

$$Ru^{III}\text{–}Ru^{II} + e^- \longrightarrow Ru^{II}\text{–}Ru^{II} \quad (6)$$

Rate of conversion of $\mathbf{1}^+ \longrightarrow$ 2 and $\mathbf{1}^+ \longrightarrow$ 1

The conversion $\mathbf{1}^+ \longrightarrow \mathbf{2}$ has been followed spectrophotometrically in dry acetonitrile solution in the temperature range 303–333 K (Fig. 9). The reaction is second order with respect to $[\mathbf{1}^+]$. Variable temperature rate constants (k) and activation parameters ($\Delta H^‡$ and $\Delta S^‡$) are listed in Table 7. The observed rate constant (k) values vary systematically with respect to L′ and follow the order $\mathbf{1c}^+ \approx \mathbf{1a}^+ > \mathbf{1b}^+$ (Table 7). The observed large enthalpy values may be ascribed to the breaking of two N–H bonds of two monomeric units (**1**) and simultaneous formation of one N–N bond in the dimer, **2**. The large negative $\Delta S^‡$ value is suggestive of an association process.[25]

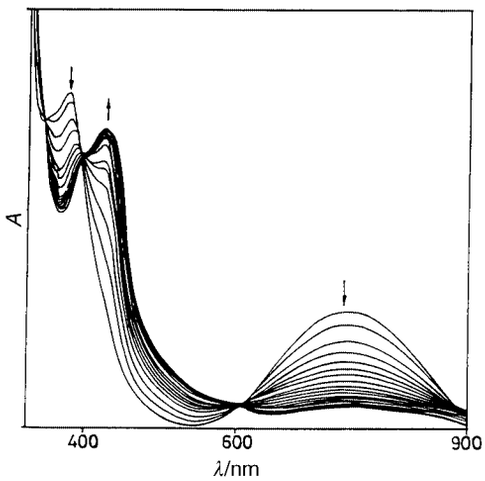

Fig. 9 Time evolution of the electronic spectra of a changing solution of $\mathbf{1b}^+ \longrightarrow$ **2b** in dry acetonitrile at 303 K. The arrows indicate increase or decrease in band intensities as the reaction proceeds.

Table 7 Rate constants and activation parameters of $\mathbf{1}^+ \longrightarrow \mathbf{2}$ and $\mathbf{1}^+ \longrightarrow \mathbf{1}$

Compound	T/K	$10^4\,k$/ $dm^3\,mol^{-1}\,s^{-1}$	$\Delta H^‡$/ $kJ\,mol^{-1}$	$\Delta S^‡$/ $J\,K^{-1}\,mol^{-1}$
(*a*) $\mathbf{1}^+ \longrightarrow \mathbf{2}$ in dry acetonitrile solution				
$\mathbf{1a}^+$	303	1.6	62.79	−47.47
	318	5.4		
	333	18.2		
$\mathbf{1b}^+$	303	2.1	64.79	−43.40
	318	7.0		
	333	24.4		
$\mathbf{1c}^+$	303	2.4	54.30	−58.03
	318	7.6		
	333	20.6		
(*b*) $\mathbf{1}^+ \longrightarrow \mathbf{1}$ in acetonitrile solution ($10^4\,k'/s^{-1}$)				
$\mathbf{1a}^+$	303	0.3	35.9	−91.9
	318	0.7		
	333	1.3		
$\mathbf{1b}^+$	303	0.25	32.55	−97.93
	318	0.52		
	333	0.90		
$\mathbf{1c}^+$	303	0.7	25.53	−104.37
	318	1.2		
	333	1.9		

The electron-transfer process $\mathbf{1}^+ \longrightarrow \mathbf{1}$ in the presence of ordinary acetonitrile has also been monitored spectrophotometrically in the temperature range 303–333 K (Fig. 10). The conversion process is first order with respect to $[\mathbf{1}^+]$. The rate constant (k') values and activation parameters ($\Delta H^‡$ and $\Delta S^‡$) are listed in Table 7. The observed rate constant (k') varies systematically depending on the nature of L′ in $\mathbf{1}^+$, following the order $\mathbf{1c}^+ > \mathbf{1a}^+ > \mathbf{1b}^+$ (Table 7). This implies superior stability of the trivalent ruthenium(III) state in $\mathbf{1b}^+$. The E°_{298} values of the ruthenium(III)–ruthenium(II) couple also follow the order **1c** > **1a** > **1b**. Thus the trends of k and E°_{298} values are internally consistent. The observed high negative entropy value (≈100 J) is not clearly understood, however the participation of a solvent molecule in the electron-transfer process ($\mathbf{1}^+ \longrightarrow \mathbf{1}$) may account for the observed kinetic behaviour.

Conclusion

We have observed the cleavage of N–N and N–C (aliphatic and aromatic) bonds of the binucleating imine functionalities (H_2L^1–H_2L^{12}) in contact with a $Ru(bpy)_2$ core. This in turn leads to the formation of complexes of the type $[Ru(bpy)_2L']$-ClO_4 **1** where L′ corresponds to the stable imine functions

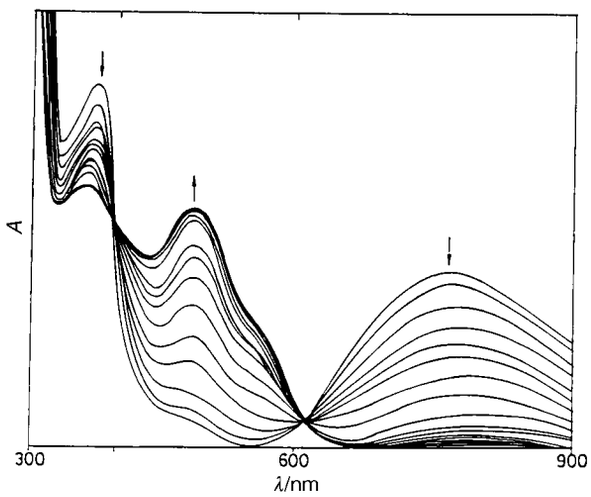

Fig. 10 Time evolution of the electronic spectra of a changing solution of $\mathbf{1b}^+ \longrightarrow \mathbf{1b}$ in ordinary acetonitrile at 303 K. The arrows indicate increase or decrease in band intensities as the reaction proceeds.

$^-OC_6H_3(R)C(R')$=NH incorporating the rare C=NH fragment. The complexes are susceptible to successive metal and ligand based redox processes and display moderately strong emission from the lowest energy MLCT bands. The electrochemically oxidised one-electron paramagnetic ruthenium(III) species, $[Ru^{III}(bpy)_2L']^{2+}$ $\mathbf{1}^+$, is found to be unstable, slowly changing to a dinuclear species of the type $[(bpy)_2Ru^{III}\{^-OC_6H_3(R)C(R')$=NN=$C(R')C(R)C_6H_3O^-\}Ru^{III}(bpy)_2]^{4+}$ **2** where the ruthenium(III) centres are antiferromagnetically coupled. In contact with a water source both complexes $\mathbf{1}^+$ and **2** return to the parent bivalent species **1**.

Experimental

Materials

The starting complex *cis*-$[Ru(bpy)_2Cl_2]\cdot 2H_2O$ was prepared according to the reported procedures.[26] Benzidine and α,α′-diamino-*p*-xylene were obtained from Fluka, Switzerland. Other chemicals and solvents were of reagent grade used as received. For electrochemical studies HPLC-grade acetonitrile was used. Commercial tetraethylammonium bromide was converted into pure tetraethylammonium perchlorate by following an available procedure.[27]

Physical measurements

Solution electrical conductivity was checked using a Systronic 305 conductivity bridge, Electronic spectra were recorded using a Shimadzu UV-2100 spectrophotometer, infrared spectra on a Nicolet spectrophotometer with samples prepared as KBr pellets. Magnetic susceptibility was checked with a PAR vibrating sample magnetometer. ^{1}H NMR spectra were obtained using a 300 MHz Varian FT-NMR spectrometer. Cyclic voltammetric and coulometric measurements were carried out using a PAR model 273A electrochemistry system. A platinum working electrode, platinum wire auxiliary electrode and SCE reference electrode were used in a three-electrode configuration. The supporting electrolyte was NEt_4ClO_4 and the concentration of the solution was $\approx 10^{-3}$ mol dm^{-3}. The half-wave potential E°_{298} was set equal to $0.5(E_{pa} + E_{pc})$, where E_{pa} and E_{pc} are anodic and cathodic cyclic voltammetric peak potentials, respectively. The scan rate used was 50 mV s^{-1}. A platinum wire gauge working electrode was used in coulometric experiments. All electrochemical experiments were carried out under a dinitrogen atmosphere and are uncorrected for junction potentials. Elemental analyses were carried out using a Perkin-Elmer 240C elemental analyser. Solution emission properties were checked using a SPEX-fluorolog spectrofluorometer.

Table 8 Crystallographic data for $[Ru^{II}(bpy)_2(L')]ClO_4\cdot CH_3CN$ **1a**

Formula	$C_{29}H_{25}ClN_6O_5Ru$
M	674.07
Crystal symmetry	Monoclinic
Space group	$P2_1/n$
a/Å	9.220(10)
b/Å	19.906(3)
c/Å	15.722(3)
β/°	90.760(10)
U/Å^3	2885.3(8)
Z	4
T/K	296
μ/mm^{-1}	0.686
Reflections collected	5405
Unique reflections (R_{int})	5052 (0.0062)
$R1$	0.052
$wR2$	0.200

Treatment of EPR data

An outline of the procedure can be found in our recent publications.[28] We note that a second solution also exists that is different from the chosen one, having small distortions and ν_1 and ν_2 values. The experimentally observed near-IR results clearly eliminate this solution as unacceptable.

Kinetic measurements

The conversions $\mathbf{1}^+ \longrightarrow \mathbf{2}$ and $\mathbf{1}^+ \longrightarrow \mathbf{1}$ were monitored spectrophotometrically in thermostatted cells. For the determination of k, the decrease in absorptions (A_t) at 790 nm for complex $\mathbf{1a}^+$, 748 nm for $\mathbf{1b}^+$ and 680 nm for $\mathbf{1c}^+$ were recorded as a function of time (t). A_∞ were measured when the intensity changes levelled off. Values of the second order rate constant, k, for the process $\mathbf{1}^+ \longrightarrow \mathbf{2}$ were obtained from the slopes of linear least-squares plots of $x/(a_0 - x)$ against t, where a_0 is the initial concentration of $\mathbf{1}^+$ and x the amount of **1** that has disappeared in time t. Values of first order rate constant, k', for the process $\mathbf{1}^+ \longrightarrow \mathbf{1}$ were obtained from the slopes of linear least-squares plots of $-\ln(A_0 - A_t)$ against t. The activation parameters $\Delta H^\ddagger$ and $\Delta S^\ddagger$ were determined from the Eyring plot.[29]

Preparation of ligands H_2L^{1-12} and complexes $[Ru(bpy)_2(L')]ClO_4$ 1a–1c

The ligands H_2L^{1-12} were prepared by condensing an appropriate salicylaldehyde with an appropriate diamine in a 2 : 1 mol ratio in dry ethanol with stirring and recrystallised from hot ethanol. The microanalytical data of the ligands are given in the Supplementary Table. The complexes **1a**–**1c** were synthesized by following a general procedure and yields varied in the range 60–65%. Details are given for one representative, **1a**.

The starting complex $[Ru(bpy)_2Cl_2]\cdot 2H_2O$ (300 mg, 0.57 mmol) and $AgClO_4$ (240 mg, 1.17 mmol) were heated to reflux in ethanol (25 cm^3) with stirring for 1 h. The orange solution of the resulting $[Ru(bpy)_2(EtOH)_2]^{2+}$ was then cooled and filtered through a Gooch (G-4) sintered-glass funnel. The ligand H_2L^1 (0.098 mg, 0.285 mmol) was then added to the above filtrate (ethanolato species). The resulting mixture was heated to reflux under a N_2 atmosphere overnight and then cooled. The precipitate thus formed was filtered off and washed thoroughly with cold ethanol. Finally, the product was recrystallised from acetonitrile–benzene (1 : 3 v/v). The yield was 60%.

CAUTION: perchlorate salts of metal complexes are generally explosive. Care should be taken while handling them.

Crystallography

Single crystals of the complex **1** were grown by slow diffusion of an acetonitrile solution of it in benzene followed by slow evaporation. Significant crystal data and data collection

parameters are listed in Table 8. Absorption correction was done by performing ψ-scan measurement.[30] The data reduction was done by using MAXUS and structure solution and refinement using the program SHELXS 93 and SHELXL 97 respectively.[31] The metal atom was located from the Patterson map and the other non-hydrogen atoms emerged from successive Fourier synthesis. The structure was refined by full-matrix least squares on F^2. All non-hydrogen atoms were refined anisotropically. Hydrogen atoms were included in calculated positions.

CCDC reference number 186/2038.

See http://www.rsc.org/suppdata/dt/b0/b001663m/ for crystallographic files in .cif format.

Acknowledgements

Financial support received from the Department of Science and Technology, New Delhi, India, is gratefully acknowledged. The structural study was carried out at the National Single Crystal Diffractometer Facilities, Indian Institute of Technology, Bombay. Special acknowledgement is made to Regional Sophisticated Instrumental Center, RSIC, Indian Institute of Technology, Bombay for providing NMR and EPR facilities. The suggestions of the Reviewers at the revision stage were very helpful.

References

1 C. M. Hartshorn, N. Daire, V. Tondreau, B. Loeb, T. J. Meyer and P. S. White, *Inorg. Chem.*, 1999, **38**, 3200; A. H. Velders, A. C. G. Hotze, J. G. Haasnoot and J. Reedijk, *Inorg. Chem.*, 1999, **38,** 2762; S. Baitalik, U. Florke and K. Nag, *Inorg. Chem.*, 1999, **38,** 3296; A. Harriman, M. Hissler, A. Khatyr and R. Ziessel, *Chem. Commun.*, 1999, 735; Ya. Xiong, X. F. He, X. H. Zon, J. Z. Wu, X. M. Chen, L. N. Ji, R. H. Li, J. Y. Zhon and K. B. Yu, *J. Chem. Soc.*, *Dalton Trans.*, 1999, 19; S. Chakraborty, P. Munshi and G. K. Lahiri, *Polyhedron*, 1999, **18**, 1437; K. D. Keerthi, B. K. Santra and G. K. Lahiri, *Polyhedron*, 1998, **17**, 1387; S. S. Kulkarni, B. K. Santra, P. Munshi and G. K. Lahiri, *Polyhedron*, 1998, **17**, 4365; T. E. Keyes, R. J. Forsters, P. M. Jayaweera, C. G. Coates, J. J. McGarvey and J. G. Vos, *Inorg. Chem.*, 1998, **37**, 5925; T. E. Keyes, P. M. Jayaweera, J. J. McGravey and J. G. Vos, *J. Chem. Soc.*, *Dalton Trans.*, 1997, 1627; J. A. Bolger, G. Ferguson, J. P. James, C. Long, P. McArdle and J. G. Vos, *J. Chem. Soc.*, *Dalton Trans.*, 1993, 1577; C. A. Howard and M. D. Ward, *Angew. Chem.*, *Int. Ed. Engl.*, 1992, **31**, 1028; J. A. Gilbert, D. S. Eggleston, W. R. Murphy, Jr., D. A. Gaselowitz, S. W. Gersten, D. J. Hodgson and T. J. Meyer, *J. Am. Chem. Soc.*, 1985, **107**, 3855.

2 V. Balzani, A. Juris, M. Venturi, S. Campagna and S. Serroni, *Chem. Rev.*, 1996, **96**, 759; A. Harriman and R. Ziessel, *Chem. Commun.*, 1996, 1707; M. D. Ward, *Chem. Soc. Rev.*, 1995, 121; D. Gust, T. A. Moore and L. Moore, *Acc. Chem. Res.*, 1993, **115**, 5975; B. O'Regan and M. Gratzel, *Nature* (*London*), 1991, **353**, 738.

3 P. Choudhuri, *Proc. Indian Acad. Sci.* (*Chem. Sci.*), 1999, **111**, 397.

4 B. M. Holligan, J. C. Jeffery, M. K. Norgett, E. Schatz and M. D. Ward, *J. Chem. Soc.*, *Dalton Trans.*, 1992, 3345.

5 N. Bag, A. Pramanik, G. K. Lahiri and A. Chakravorty, *Inorg. Chem.*, 1992, **31**, 40.

6 V. R. L. Constantino, H. E. Toma, L. F. C. de Oliveira, F. N. Rein, R. C. Rocha and D. O. Silva, *J. Chem. Soc.*, *Dalton Trans.*, 1999, 1735.

7 P. Bernhard, H. B. Burgi, J. Hauser, H. Lehmann and A. Ludi, *Inorg. Chem.*, 1982, **21**, 3936.

8 N. Bag, S. B. Choudhury, A. Pramanik, G. K. Lahiri and A. Chakravorty, *Inorg. Chem.*, 1990, **29**, 5014.

9 N. Bag, S. B. Choudhury, G. K. Lahiri and A. Chakravorty, *J. Chem. Soc.*, *Chem. Commun.*, 1990, 1626.

10 A. R. Chakravarty, A. Chakravorty, F. A. Cotton, L. R. Falvello, B. K. Ghosh and M. Thomas, *Inorg. Chem.*, 1983, **22**, 1892.

11 D. Nasipuri, *Stereochemistry of Organic Compounds*, Wiley Eastern Limited, New Delhi, 1994, p. 81.

12 M. H. Kuchama, T. Nicholson, A. Davison, W. M. Davis and A. G. Jones, *Inorg. Chem.*, 1997, **36**, 3237.

13 B. J. Coe, T. J. Meyer and P. S. White, *Inorg. Chem.*, 1995, **34**, 593; W. Paw, W. B. Connick and R. Eisenberg, *Inorg. Chem.*, 1998, **37**, 3919; R. Alsfasser and R. V. Eldik, *Inorg. Chem.*, 1996, **35**, 628.

14 G. M. Brown, T. R. Weaver, F. R. Keene and T. J. Meyer, *Inorg. Chem.*, 1976, **15**, 190.

15 B. K. Santra, M. Menon, C. K. Pal and G. K. Lahiri, *J. Chem. Soc.*, *Dalton Trans.*, 1997, 1387.

16 L. M. Vogler and K. J. Brewer, *Inorg. Chem.*, 1996, **35**, 818.

17 G. A. Crosby and W. H. Elfring, Jr., *J. Phys. Chem.*, 1976, **80**, 2206.

18 J. V. Houten and R. J. Watts, *J. Am. Chem. Soc.*, 1976, **98**, 4853; E. F. Godefroi and E. L. Little, *J. Org. Chem.*, 1956, **21**, 1163; P. Chen, R. Duesing, D. K. Graff and T. J. Meyer, *J. Phys. Chem.*, 1991, **95**, 5850.

19 N. Bag, G. K. Lahiri, S. Bhattacharya, L. R. Falvello and A. Chakravorty, *Inorg. Chem.*, 1988, **27**, 4396; G. K. Lahiri, S. Bhattacharya, S. Goswami and A. Chakravorty, *J. Chem. Soc.*, *Dalton Trans.*, 1990, 561.

20 S. Goswami, R. N. Mukherjee and A. Chakravorty, *Inorg. Chem.*, 1983, **22**, 2825; B. K. Ghosh and A. Chakravorty, *Coord. Chem. Rev.*, 1989, **95**, 239.

21 N. Bag, G. K. Lahiri, P. Basu and A. Chakravorty, *J. Chem. Soc.*, *Dalton Trans*., 1992, 113; A. Pramanik, N. Bag, G. K. Lahiri and A. Chakravorty, *J. Chem. Soc.*, *Dalton Trans.*, 1990, 3823.

22 N. J. Hill, *J. Chem. Soc.*, *Faraday Trans.*, 1972, 427; B. Bleaney and M. C. M. O'Brien, *Proc. Phys. Soc.*, *London*, *Sect. B*, 1956, **69**, 1216; J. S. Griffith, *The Theory of Transition Metal Ions*, Cambridge University Press, London, 1972, p. 364; C. Daul and A. Goursot, *Inorg. Chem.*, 1985, **24**, 3354; B. K. Santra and G. K. Lahiri, *J. Chem. Soc.*, *Dalton Trans.*, 1997, 129; R. Hariram, B. K. Santra and G. K. Lahiri, *J. Organomet. Chem.*, 1997, **540**, 155; C. J. Ballhausen, *Introduction to Ligand Field Theory*, McGraw-Hill, New York, 1962, p. 99.

23 E. M. Kober and T. J. Meyer, *Inorg. Chem.*, 1983, **22**, 1614; G. K. Lahiri, S. Bhattacharya, M. Mukherjee, A. K. Mukherjee and A. Chakravorty, *Inorg. Chem.*, 1997, **26**, 3359.

24 A. Bharath, B. K. Santra, P. Munshi and G. K. Lahiri, *J. Chem. Soc.*, *Dalton Trans.*, 1998, 2643; C. Trindle and S. N. Datta, *Int. J. Quantum Chem.*, 1996, **57**, 781.

25 K. D. Laidler, *Chemical Kinetics*, Tata-McGraw-Hill, New Delhi, 1980.

26 B. P. Sullivan, D. J. Salmon and T. J. Meyer, *Inorg. Chem.*, 1978, **17**, 3334.

27 D. T. Sawyer, A. Sobkowiak and J. L. Roberts, Jr., *Electrochemistry for Chemists*, Wiley, New York, 1995.

28 P. Munshi, R. Samanta and G. K.Lahiri, *J. Organomet. Chem.*, 1999, **586**, 176.

29 R. G. Wilkins, *The Study of Kinetics and Mechanism of Reactions of Transition Metal Complexes*, Allyn and Bacon, Boston, MA, 1974.

30 A. C. T. North, D. C. Phillips and F. S. Mathews, *Acta Crystallogr.*, *Sect. A*, 1968, **24**, 351.

31 G. M. Sheldrick, SHELXTL, Version 5.03, Siemens Analytical X-ray Instruments Inc., Madison, WI, 1994.